Development of an Inertial Measurement Unit for Unmanned Aerial Vehicles

Khaled S. Hatamleh[*], Angel Flores-Abad, Pu Xie, Gerardo Martinez, Brandi Herrera and Ou Ma

[a] Department of Mechanical & Aerospace Engineering, New Mexico State University, Las Cruces, New Mexico, USA

Abstract

Unmanned Aerial Vehicles (UAVs) are being deployed in a vast variety of military, civilian, industrial and agricultural applications. Dynamics modeling is an essential step towards designing autonomous controllers for UAV systems. The dynamics modeling on the other hand requires accurate records of the UAVs motion states during real flight tests, this is usually achieved using Inertial Measurement Units (IMUs) and other necessary sensors. This work introduces the purpose, the development and the calibration details of a special six degrees of freedom IMU. The unit is being used in verifying an online UAV dynamics model parameter estimation methodology.

Keywords: IMU, UAV dynamics models, parameter estimation, calibration.

1. Introduction

The extensive use of UAVs demands some kind of manual (highly skilled pilot crew) or autonomous control to be present along. This causes UAVs to be really expensive, and creates a challenge for scientists to design a reliable controller and to develop appropriate means to safely validate the designed controllers without crashing the involved UAVs.

Most of the controllers are dynamics model based. Figure 1 illustrates that the accuracy of a UAV dynamics model depends on the mathematical formulation and on the values of the model's parameters. If the UAV dynamics model changes for any reason during flight (fuel mass loss, or aerodynamic disturbances from wind gusts), the model based controller will not perform as intended. To overcome this problem an on-line dynamics model parameter estimation [1]. The method updates the hanging values of the UAV dynamics model parameters during flight, leading into a more accurate dynamics model and a better flight control quality. More over the estimation method will provide a more realistic offline UAV dynamics model, that can serve as a safe & reliable tool to ensure that the designed controller works properly, minimizing the possibility of crashing the real modeled UAV.

The previous shows the value an accurate UAV dynamics model can add to the UAV control design and test processes. Experimentally dynamics modeling requires motion state records of the dynamic system under investigation; this includes records of position, velocity,
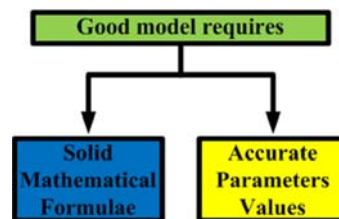

Figure 1. Characteristics of a good dynamics model.

angular rate, acceleration, angular accelerations, altitude, pressure, etc. The motion states are obtained using the appropriate sensors and sensory units like Inertial Navigation Systems (INS) and IMUs.

IMUs are electronic devices that are capable of providing three dimensional velocity and acceleration information of the vehicle they are installed on at high sampling rates. They consist of three accelerometers and three gyroscopes mounted in a set of three orthogonal axes [2]. IMUs were expensive in general until the recent development of cheap ceramic and silicon sensors, which has lowered their price and the quality of their measurements. Nowadays IMUs are available at a lower cost, they can be even developed using off-the-shelf components. The major problems encountered with such developed cheap IMUs, are the need to perform the calibration process for the used sensors, and the need to filter the existing noise at the output signals due vibrations and measurements noise. This work will describe the development of a special 6-DOF IMU board to conduct an experimental research study over a special 2-DOF helicopter system. The paper also introduces the calibration procedures and results of the IMU sensors.

*Corresponding author. kshh@nmsu.edu

2. Why custom designed IMU?

Prior to the development of this work, an early study [1] introduced a method to model, and estimates the unknown model parameters of a general 6-DOF flying rigid body. The method is being verified experimentally by means of a 2-DOF helicopter system manufactured by Quanser® and shown in Figure 2. The method requires records of the helicopter position, angular velocity and angular acceleration information in a continuous online manner. The original helicopter system is equipped with a pair of encoders to feedback the angular position information around the pitch and the yaw degrees of freedom which are termed (θ) and (ψ) respectively. The system was modified extensively to be able to provide the angular rate ($\dot\theta$, $\dot\psi$) and angular acceleration ($\ddot\theta$, $\ddot\psi$) information, details of the system and the modifications done are described by an earlier work of the authors[3].

To be able to provide the necessary motion state information, the first derivative of the encoder's signals can be considered to obtain the angular speeds, while the second derivative produces the angular accelerations. This has been proved inefficient and inaccurate due to error propagation through the first and second derivatives. This made it necessary to use sensors that are able to provide the needed motion states. The angular rate information can be obtained directly using two dual-axis rate gyro sensors. However the case is not as simple for the angular accelerations. There are few sensors that are able to provide measurements of the angular acceleration directly, and those are generally expensive, if attainable. Moreover they represent newly developed technologies that have not been proven efficient yet. The previous made it inevitable to follow an indirect method to measure the angular accelerations. A method that relies on the general relative linear acceleration equation has been proposed. It requires the knowledge of the local acceleration components of at least three different points, of known relative positions, fixed at a rigid body of known angular speed. Therefore three tri-axis linear accelerometers and the two dual-axis rate gyros shall be used to achieve the mission. A detailed derivation and analysis of the indirect angular acceleration measurement is described by Appendix A or reference 3. Most of the commercially available IMUs are equipped with one tri-axis accelerometer, which doesn't satisfy the
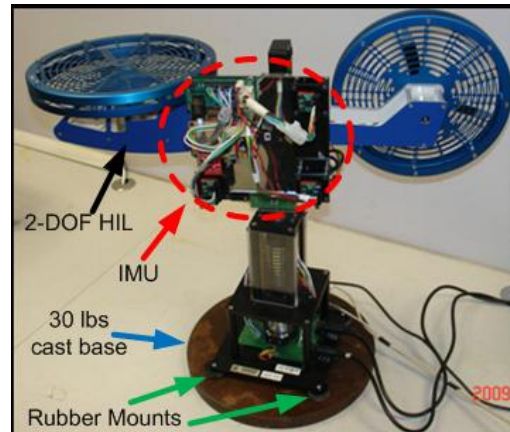

Figure 2. Quanser's modified 2-DOF helicopter

requirements of the indirect angular acceleration method proposed. This has lead into performing a costume designed 6-DOF IMU system; this is the lowest price solution, and the most suited for the adopted indirect angular acceleration method. The rest of the paper will describe the IMU's components, structure, and calibration process.

3. Components & Structure

The IMU system shown by Figure 3 consists of a Plexiglas base that holds three (LIS3LV02DQ) tri-axis accelerometers[4], one ±300(◦\sec) dual axis (LPY530AL) rate gyro[6], one ±300(◦\sec) dual axis (LPR530AL) rate gyro[5], a single (PIC24FJ64GA002) microprocessor board, a Li-Po (7.4 Volts, 1300 mhA) battery, X-Bee wireless serial connection and additional interfacing circuits. The developed IMU system functional flow block diagram is illustrated by Figure 4; the 7.4 Volts Lithium Polymer (LiPo) Battery is connected to an interfacing circuit that modulates the voltage into a level that is suitable to power all board components. The three tri-axis accelerometers communicate with the microcontroller through SPI bus channel.
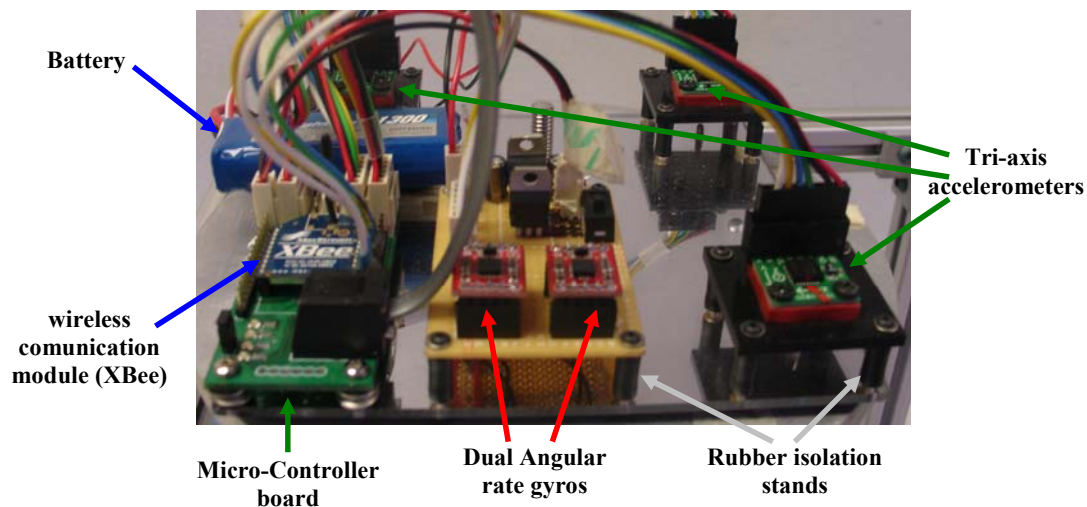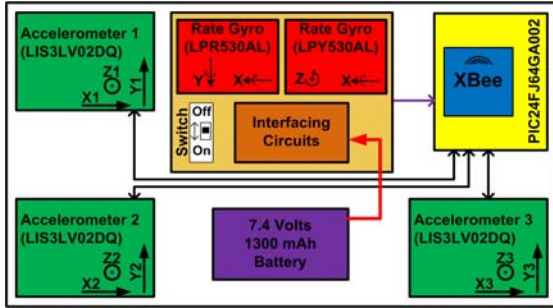

Figure 3. IMU system components

Figure 4. IMU schematic diagram.

The two dual axis rate gyros output is connected to the ADC input channels of the PIC microcontroller. The XBee installed over the microcontroller board sends all the gathered information via a wireless (57600) baud rate serial connection into a stationary PC or laptop where the information are saved as text files.

The Information gathered by the IMU are saved as series of 32 bytes long hexadecimal data frames; each frame contains the acceleration components along the sensitivity axes $(\ddot{x}_k, \ddot{y}_k, \ddot{z}_k)$ of each of the three tri-axis accelerometers, (k = 1, 2, 3), every accelerometer reserves 6 bytes of the total frame size. In addition the frame contains the angular velocity readings of the two dual-axis rate gyros followed by the frame sample time; 4 bytes are required for each dual-axis rate gyro while 2 bytes are needed for the sample time. The data frame starts with the Hex number (0x4141) (2 bytes) and ends by the Hex number (0x5A5A) (another 2 bytes). A successful data frame will look similar to the one shown at Figure 5. The IMU is capable of providing the motion states of the UAV at a sampling frequency of about 56 HZ, the gathered text files are processed by a MATLAB® code to convert the hexadecimal information and extract the motion states.

4. IMU Calibration

Because the sensors used to build the IMU are off the shelf components, the performance and accuracy is not guaranteed unless a precise calibration process is performed. The calibration was done for all accelerometers sensors and the two dual axis rate gyros. The procedures followed are similar to those found in [7-8]; where a linear model (shown in Figure 6) of the accelerometer and the rate gyros was assumed. An illustration of the modeling equations, procedures and equipments used during the
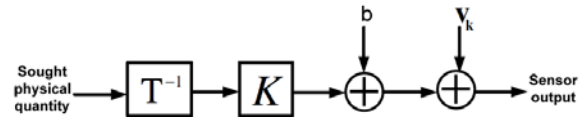

Figure 6. Sensor linear model.

accelerometer and rate gyro calibration is described shortly.

4.1 Accelerometer Calibration

According to the assumed linear model one can write the measured acceleration at an accelerometer local frame (sensitivity axes coordinates) as:

$$\tilde{\mathbf{s}}^{ak} = \mathbf{K}_{ak}\mathbf{s}^{ak} + \mathbf{b}_{ak} + \mathbf{v}_{ak} \tag{1}$$

where $\tilde{\mathbf{s}}^{ak}$ is the (3x1) output vector of accelerometer k, (k = 1, 2 and 3) that represents the local acceleration components along the sensor's sensitivity axes coordinates $\begin{bmatrix} a_{kx} & a_{ky} & a_{kz} \end{bmatrix}^T$, $\mathbf{v}_{ak}$ is the measurement noise term, $\mathbf{K}_{ak}$ is the (3x3) diagonal scale factor matrix that includes the scaling factors along each of the three sensitivity axes of accelerometer k. $\mathbf{K}_{ak} = diag(k_{akx}, k_{aky}, k_{akz})$, $\mathbf{b}_{ak}$ is the (3x1) bias vector along accelerometer k sensitivity axes $\mathbf{b}_{ak} = \begin{bmatrix} b_{akx} & b_{aky} & b_{akz} \end{bmatrix}^T$ and $\mathbf{s}^{ak}$ is the (3x1) vector of the real acceleration components present at accelerometer k local frame. Prior calibration the values of $\mathbf{K}_{ak}$, $\mathbf{b}_{ak}$ and $\mathbf{v}_{ak}$ are all unknown, on the other hand the values of $\tilde{\mathbf{s}}^{ak}$ are obtained directly from the accelerometer reading. The $\mathbf{s}^{ak}$ term or the so called reference acceleration values are assumed to be known as they are controlled by the experimental setup of the calibration process. The purpose of the calibration process is to estimate the values of $\mathbf{K}_{ak}$, $\mathbf{b}_{ak}$ and $\mathbf{v}_{ak}$, this usually needs a set of different accelerometer readings that accompanies different applied well defined reference acceleration values. The Earth field of gravity was used as the well known reference acceleration value.
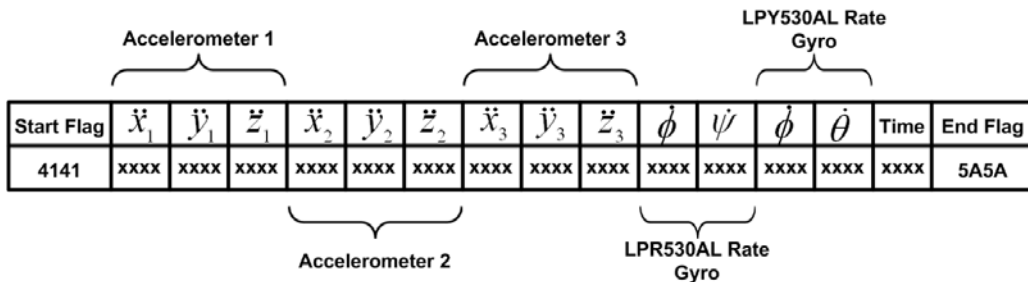

Figure 5. Schematic of the IMU data frame.

Figure 7. Accelerometer calibration

A tri-axis accelerometer was fixed into precise rotating table (accelerometer calibration platform) that can be turned into any angular position with minutes accuracy by means of a manual handle (See Figure 7). The concept is simple, if an accelerometer is attached to the previously mentioned rotating table as shown by Figure 8, the accelerometer x-axis (pointing up in position-1) should theoretically read $(-g)$ because the gravity field acceleration lies totally along the negative x-axis of the accelerometer. If the table with the attached sensor is rotated into a new angular position such that the gravity field acceleration is at angle θ_r with the x-axis (position-2 of Figure 8), then the value of the gravity field acceleration acting along the x axis reading is defined as ($\mathbf{g}_x = \mathbf{g}\cos\theta_r$).

The calibration platform with the attached IMU board was rotated into 37 different static locations starting from the position $0°$ into the position $180°$ by an increment of $5°$ each time (see Figure 9). The values of the x-axis sensor readings at each static position of the 37 were recorded. The same procedures were repeated for the y and the z axes after flipping the IMU board in a proper orientation such that the axis of concern is pointing up at the initial angular position of the data gathering process. This whole process was done for all three tri-axis accelerometers using the same rotating table and under the same operating temperature. Ignoring the noise term in equation (1):

$$\tilde{\mathbf{s}}^{ak} = \mathbf{K}_{ak}\mathbf{s}^{ak} + \mathbf{b}_{ak}$$

$$\begin{bmatrix} \tilde{\mathbf{s}}_x^{ak} \\ \tilde{\mathbf{s}}_y^{ak} \\ \tilde{\mathbf{s}}_z^{ak} \end{bmatrix} = \begin{bmatrix} k_{akx} & 0 & 0 \\ 0 & k_{aky} & 0 \\ 0 & 0 & k_{akz} \end{bmatrix} \begin{bmatrix} \mathbf{s}_x^{ak} \\ \mathbf{s}_y^{ak} \\ \mathbf{s}_z^{ak} \end{bmatrix} + \begin{bmatrix} b_{akx} \\ b_{aky} \\ b_{akz} \end{bmatrix} \qquad (2)$$
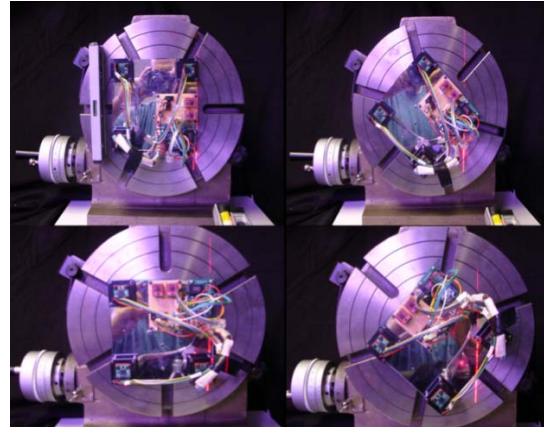

Figure 9. **IMU** board on accelerometer calibration platform at different angular positions.

which can be rewritten into:

$$\begin{bmatrix} \mathbf{s}_x^{ak} & 0 & 0 & 1 & 0 & 0 \\ 0 & \mathbf{s}_y^{ak} & 0 & 0 & 1 & 0 \\ 0 & 0 & \mathbf{s}_z^{ak} & 0 & 0 & 1 \end{bmatrix} \begin{bmatrix} k_{akx} \\ k_{aky} \\ k_{akz} \\ b_{akx} \\ b_{aky} \\ b_{akz} \end{bmatrix} = \begin{bmatrix} \tilde{\mathbf{s}}_x^{ak} \\ \tilde{\mathbf{s}}_y^{ak} \\ \tilde{\mathbf{s}}_z^{ak} \end{bmatrix} \qquad (3)$$

For each accelerometer the recorded data during the calibration process at each angular position is stacked into a similar format of Equation (3) (this requires data from x, y and z sensitivity axes of accelerometer k for the same angular position from all three different sensor board orientations), then the results of all 37 angular positions are stacked into a linear regression format of $(\boldsymbol{\beta}_k \mathbf{r}_k = \mathbf{s}_k)$; where $\mathbf{r}_k$ is the vector that contains all the unknown scale factors and bias values of accelerometer k, $\mathbf{s}_k$ is the acceleration values recorded above by accelerometer k sensitivity axes at all angular positions and $\boldsymbol{\beta}_k$ contains the values of the known reference signal applied along the sensitivity axes of sensor k during calibration process at all according angular positions and calculated by Equation (1). The linear regression form can be solved for $\mathbf{r}_k$ using least squares technique; i.e; ($\mathbf{r}_k = \boldsymbol{\beta}_k^{+1}\mathbf{s}_k$). Results of the calibration process can be used to calculate the real applied acceleration value along any sensor sensitivity axes using a manipulated version of Equation (2):

Figure 8. Schematic of a tri-axis accelerometer on the rotating table

$$\mathbf{s}^{ak} = \mathbf{K}_{ak}^{-1}\left(\tilde{\mathbf{s}}^{ak} - \mathbf{b}_{ak}\right) \qquad (4)$$

4.2 Rate Gyro Calibration

Applying the same linear sensor model over the rate gyro sensors produces:

$$\tilde{\boldsymbol{\omega}}_g^g = \mathbf{K}_g \boldsymbol{\omega}_g^g + \mathbf{b}_g + \mathbf{v}_g \qquad (5)$$

where $\tilde{\boldsymbol{\omega}}_g^g$ is the (3x1) angular rate output vector of all single-axis angular rate sensors, $\boldsymbol{\omega}_g^g$ is the (3x1) vector of the real angular rate applied along the non-orthogonal sensitivity coordinate axes of all single-axis angular rate sensors, $\mathbf{K}_g$ is the (3x3) diagonal scale factor matrix that includes the three scaling factors along each sensor sensitivity axis, $\mathbf{K}_g = diag(k_{gx}, k_{gy}, k_{gz})$, $\mathbf{b}_g$ is the (3x1) bias vector of all angular rate sensors, $\mathbf{b}_g = \begin{bmatrix} b_{gx} & b_{gy} & b_{gz} \end{bmatrix}^T$ and $\mathbf{v}_g$ is the angular rate measurement noise term.

The rate gyros calibration process needs a set of different rate gyros readings for different applied reference angular rate values. The reference signal was attained by means of custom designed PI-controlled angular rotational platform designed by the research group members, the table can rotate at reference angular velocities range of $\pm 4\pi/3$ (rad/sec), Figure 10. shows the prototyped table with the IMU mounted on top of the rotary flat disk. Records of angular speed read by the IMU were obtained as the speed of the calibration table was varied from $-4\pi/3$ (rad/sec) to $4\pi/3$ (rad/sec) by increments of $\pi/9$ (rad/sec) for each recorded set; this yeilds about 23 reference angular rate values/rate gyro readings pairs. This process was repaeted three times for the the three different IMU orientations to calibrate all rate gyro sensitivity axes. When a tri-axis angular rate sensor system built up from three single-axis angular rate sensors a non-orthogonal coordinate frame (or angular rate sensor system sensitivity axes)
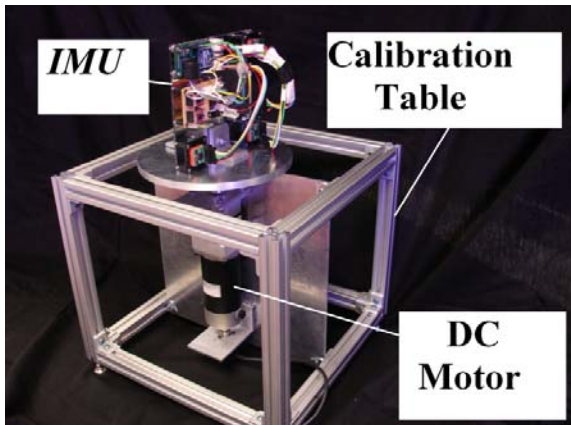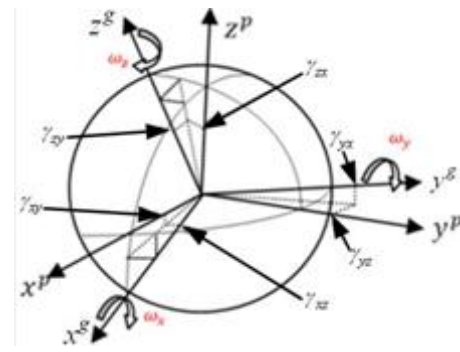

Figure 10. Rate gyro calibration platform with **IMU** on top.

(x^g, y^g, z^g) is created. Figure 11, shows this coordinate

Figure 11. Platform and rate gyro system axes frame.

system mounted on the orthogonal coordinate axes (x^p, y^p, z^p) of a platform. Due to sensors mounting imprecision, the two coordinate systems will differ by a set of six small angles. Those angles are needed to estimate the value of the angular rate measured around the non-orthogonal sensitivity axes of the angular rate sensors $\boldsymbol{\omega}_g^g$ at the orthogonal platform coordinates axes where the angular rate vector is denoted $\boldsymbol{\omega}_p^p$, the following equation maps the rate gyro reading into the platform coordinates axes[9]:

$$\boldsymbol{\omega}_p^p = \mathbf{T}_g^p \boldsymbol{\omega}_g^g, \qquad \mathbf{T}_g^p = \begin{pmatrix} 1 & -\gamma_{yz} & \gamma_{zy} \\ \gamma_{xz} & 1 & -\gamma_{zx} \\ -\gamma_{xy} & \gamma_{yx} & 1 \end{pmatrix} \qquad (6)$$

Where γ_{ij} is the rotation of the *i*-th angular rate sensor sensitivity axis around the *j*-th platform axis and $\mathbf{T}_g^p$ is the rotation matrix that maps the angular rate vector from the non-orthogonal sensitivity axes of the angular rate sensors into the platform orthogonal coordinate system[7]. Defining the platform coordinate system such that its (x^p, y^p) plane coincides with the (x^g, y^g) plane of the (LPR530AL) sensor board sensitivity axes will reduce the total number of the unknown angles down to two; $\{\gamma_{xy}, \gamma_{xz}, \gamma_{yz}, \gamma_{yx}\}$ will be zero. Equation (6) reduces to:

$$\boldsymbol{\omega}_p^p = \mathbf{T}_g^p \boldsymbol{\omega}_g^g, \qquad \mathbf{T}_g^p = \begin{pmatrix} 1 & 0 & \gamma_{zy} \\ 0 & 1 & -\gamma_{zx} \\ 0 & 0 & 1 \end{pmatrix} \qquad (7)$$

Substituting equation (7) back into equation (5) after ignoring the noise term yields:

$$\begin{bmatrix} \tilde{\omega}_x^g \\ \tilde{\omega}_y^g \\ \tilde{\omega}_z^g \end{bmatrix} = \begin{bmatrix} k_{gx} & 0 & 0 \\ 0 & k_{gy} & 0 \\ 0 & 0 & k_{gz} \end{bmatrix} \begin{bmatrix} 1 & 0 & \gamma_{zy} \\ 0 & 1 & -\gamma_{zx} \\ 0 & 0 & 1 \end{bmatrix}^{-1} \begin{bmatrix} \omega_x^g \\ \omega_y^g \\ \omega_z^g \end{bmatrix} + \begin{bmatrix} b_{gx} \\ b_{gy} \\ b_{gz} \end{bmatrix} \qquad (8)$$

This can be rewritten into:

$$
\begin{bmatrix}
\omega_x^g & -\omega_z^g & 0 & 0 & 0 & 1 & 0 & 0 \\
0 & 0 & \omega_y^g & \omega_z^g & 0 & 0 & 1 & 0 \\
0 & 0 & 0 & 0 & \omega_z^g & 0 & 0 & 1
\end{bmatrix}
\begin{bmatrix}
k_{gx} \\
k_{gx}\gamma_{zy} \\
k_{gy} \\
k_{gy}\gamma_{zx} \\
k_{gz} \\
b_{gx} \\
b_{gy} \\
b_{gz}
\end{bmatrix}
=
\begin{bmatrix}
\tilde{\omega}_x^g \\
\tilde{\omega}_y^g \\
\tilde{\omega}_z^g
\end{bmatrix}
\quad (9)
$$

The data recorded during the rate gyros calibration process will be stacked into a form similar to that shown by equation (9) at each reference speed, all 23 records from all **IMU** different rotational readings during the calibration process will be stacked into one linear regression format $(\boldsymbol{\chi}\mathbf{z} = \tilde{\boldsymbol{\omega}})$, where $\boldsymbol{\chi}$ contains 23 stacks of the matrix

$$
\begin{bmatrix}
\omega_x^g & -\omega_z^g & 0 & 0 & 0 & 1 & 0 & 0 \\
0 & 0 & \omega_y^g & \omega_z^g & 0 & 0 & 1 & 0 \\
0 & 0 & 0 & 0 & \omega_z^g & 0 & 0 & 1
\end{bmatrix},
$$

$\mathbf{z} = \begin{bmatrix} k_{gx} & k_{gx}\gamma_{zy} & k_{gy} & k_{gy}\gamma_{zx} & k_{gz} & b_{gx} & b_{gy} & b_{gz} \end{bmatrix}^T$ is the vector that contains all the unknown values to be estimated and $\tilde{\boldsymbol{\omega}}$ is the (69x1) vector that contains the stacks of the tri-axis rate gyro system readings recorded during the calibration process. The system can be easily solved for the values of $\mathbf{z}$ using the equation:

$$
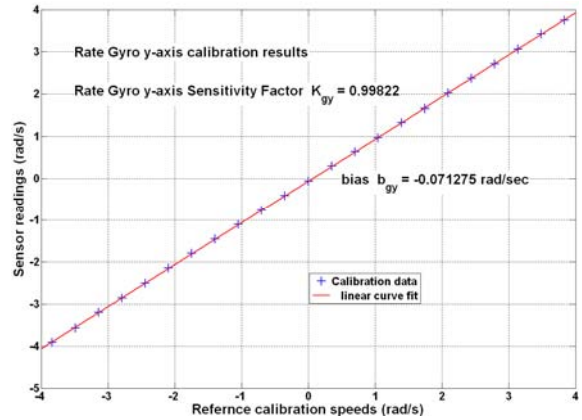\mathbf{z} = \boldsymbol{\chi}^{+1}\tilde{\boldsymbol{\omega}} \quad (10)
$$

Once the calibration process is done the readings of the angular rate sensors can be used to calculate the platform's angular rate vector using:

$$
\boldsymbol{\omega}_p^p = \mathbf{T}_g^p \mathbf{K}_g^{-1} \left(\tilde{\boldsymbol{\omega}}_g^g - \mathbf{b}_g \right) \quad (11)
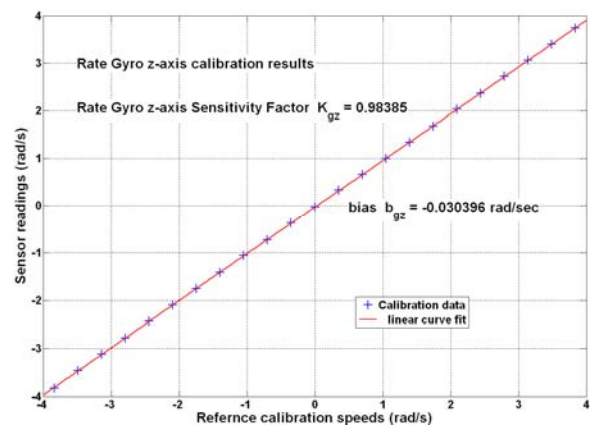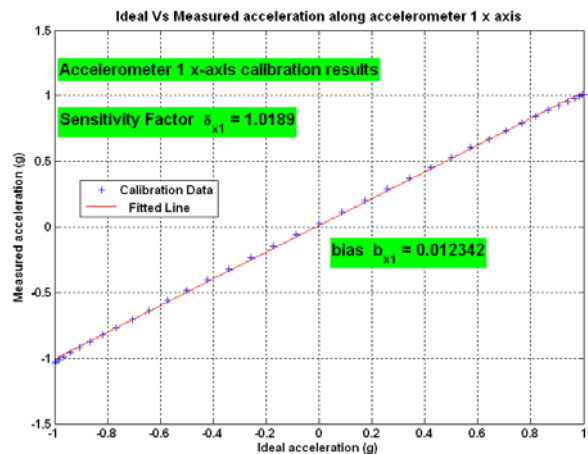$$

5. Results
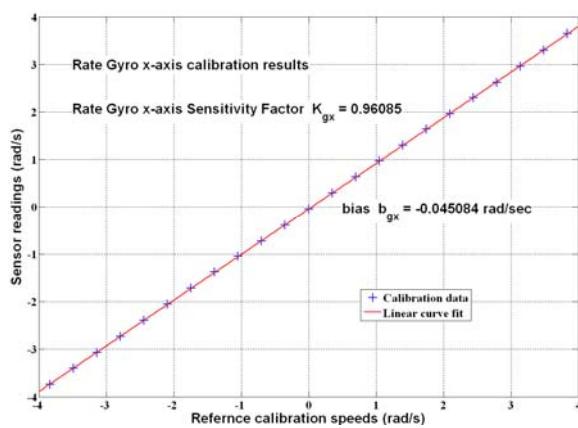
(b)

(c)

Figure 12. Rate Gyro calibration results; (a) x-axis, (b) y-axis and (c) z-axis.
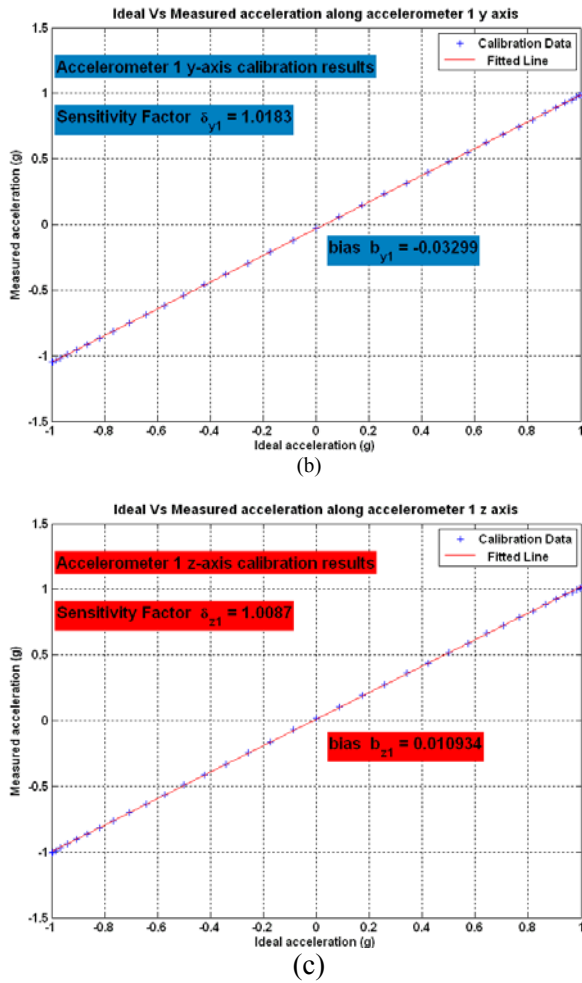

(a)

(a)

(b)

(c)

Figure 13. Accelerometer 1 calibration results along (a) x-axis, (b)
y –axis, (c) z-axis.

Figure 12 shows the calibration results of the tri-axis rate gyro system, while figure 13 shows the calibration results along all sensitivity axes of accelerometer 1. The results of all three tri axes accelerometers are summarized in Table. 1; the table shows the scaling factors and bias values for each accelerometer along the three sensitivity axes when operating at $25°$ C. Values of the scaling factors are close to one indicating the generated accelerometer reading is very close to the applied reference acceleration. The bias values on the other hand are enclosed in the range of (-0.033 to 0.0123) g. It is worthy to mention that the calibration values cannot be used if the operating temperature is different than that of the calibration process ($25°$ C). For different temperatures the calibration process has to be carried out again to extract the new scale factors and bias values.

Table 1. Accelerometers calibration process results

Accelerometer	k_{akx}	k_{aky}	k_{akz}	b_{akx} (g)	b_{aky} (g)	b_{akz} (g)
k=1	1.01	1.01	1.00	0.01	-0.03	0.01
k=2	1.02	1.01	1.01	-0.00	-0.01	0.00
k=3	1.02	1.01	1.00	-0.00	-0.019	-0.025

The rate gyros calibration process results are presented on Table. 2; the table shows values of the scaling factors, the biases and the misalignment angles of the rate gyro z-axis from the rate gyro (x-y) plane. The results are valid under ($25°$ C) operating temperature. The scale factors here are also close to one. The misalignment angles values are very small indicating a tiny physical tilt of the LPY530AL dual axis rate gyro that holds the z axis from the plane of the LPR530AL rate gyro that holds the (x-y) sensitivity axes.

Table 2. Rate gyro sensor system calibration results.

k_{gx}	k_{gy}	k_{gz}	b_{gx} (rad/s)	b_{gy} (rad/s)	b_{gz} (rad/s)	γ_{zx} (rad)	γ_{zy} (rad)
0.96	0.99	0.98	-0.04	-0.07	-0.03	-0.00	-0.01

6. Conclusions

In this work the motivation behind the need for a special IMU system is introduced. An IMU system has been built, programmed, and calibrated to be used in UAVs dynamics modeling applications. The components, structure and communication system of the developed board are described. A linear model of the used accelerometers and rate gyro sensors is assumed. The calibration process of the previously mentioned sensors has been detailed with a description of the calibration platforms and the followed experimental procedures. The calibration results are ready to be used to estimate values of real applied angular accelerations and angular rates directly as described by equations (4) and (11) respectively. The experimental verification of the indirect angular accelerometer method is in progress. The authors of the paper will further verify the IMU readings using several experimental tests prior using the IMU to experimentally verify the online UAV dynamics model parameter estimation method proposed in a previous work.

References

[1] Hatamleh, K., Ma, O. and Paz, R., "A UAV Model Parameter Identification Method: A Simulation Study", International Journal of Information Acquisition Vol. 6, No., 2009, 225–238.

[2] Dissanayake, G., Sukarieh, S., Nebto, E. and Durrant-Whyte, H. , "The Aiding Of A Low-Cost Strap Down Inertial Measurement Unit Using Vehicle Model Constraints For Land Vehicle Applications", IEEE transactions on robotics and automation, Vol. 17, No. 5, 2001,731–747.

[3] Hatamleh, K., Xie, P., Martinez, G., McAvoy, J., Ma, O., "An UAV Parameter Identification Method", AIAA Modeling & Simulation Technologies Conf. Chicago, IL, USA, 2009.

[4] STMicroelectronics Digital devices (lis3lv02dq) tri-axis accelerometer, (http://www.sparkfun.com/datasheets/IC/LIS3LV02DQ.pdf.hj).

[5] STMicroelectronics Digital devices (lpr530al) dual axis rate gyro sensor, (http://www.sparkfun.com/datasheets/Sensors/IMU/lpr530al.pdf.)

[6] STMicroelectronics Digital devices (lpy530al) dual axis rate gyro sensor. (http://www.sparkfun.com/datasheets/Sensors/IMU/lpy530al.pdf).

[7] Skog, I., and Handel, P., "Calibration of a mems inertial measurement unit", the 17th IMEKO World Congress, Rio deJaneiro, Brazil, 2006.

[8] Sahawneh, L., and Jarrah, M., A., "Development and calibration of low cost mems IMU for UAV applications", the 5th International Symposium on Mechatronics and Its Applications, ISMA, Amman, Jordan, 2008.

[9] Britting, K. R., Inertial Navigation Systems Analysis, Wiley, New York; 1971.